Escola de Camins
Escola Tècnica Superior d'Enginyeria de Camins, Canals i Ports
UPC BARCELONATECH

Study and development of a solidification model using CFD

MASTER FINAL THESIS

Final Thesis developed by:
Bazán Escoda, Aitor

Directed by:
Castilla, Robert

Master in:
Numerical methods in Engineering

Barcelona, date

Department of Fluid mechanics

UNIVERSITAT POLITÈCNICA DE CATALUNYA

MASTER THESIS

Study and development of a solidification model using CFD

Author:
Aitor BAZÁN ESCODA

Supervisor:
Dr. Robert CASTILLA

A thesis submitted in fulfillment of the requirements for the degree of Master Thesis

in the

Research Group Name
Escola Tècnica Superior d'Enginyeria de Camins, Canals i Ports de Barcelona

June 8, 2022

Declaration of Authorship

I, Aitor BAZÁN ESCODA, declare that this thesis titled, "Study and development of a solidification model using CFD" and the work presented in it are my own. I confirm that:

- This work was done wholly or mainly while in candidature for a research degree at this University.
- Where any part of this thesis has previously been submitted for a degree or any other qualification at this University or any other institution, this has been clearly stated.
- Where I have consulted the published work of others, this is always clearly attributed.
- Where I have quoted from the work of others, the source is always given. With the exception of such quotations, this thesis is entirely my own work.
- I have acknowledged all main sources of help.
- Where the thesis is based on work done by myself jointly with others, I have made clear exactly what was done by others and what I have contributed myself.

Signed:

Date:

UNIVERSITAT POLITÈCNICA DE CATALUNYA

Abstract

Faculty Name
Escola Tècnica Superior d'Enginyeria de Camins, Canals i Ports de Barcelona

Master Thesis

Study and development of a solidification model using CFD

by Aitor BAZÁN ESCODA

Phase change materials (PCMs) are of great interest within the automotive industry field. Not only when used in thermal management applications but also in different areas where these materials are of vital importance for both a safe and comfortable driving. For such objective, the present project arises from the idea of understanding solidification processes in windshield washer tanks. In this context, this master's thesis produces a comprehensive state of the art of some of the current numerical methods to effectively represent water solidification.

An OpenFOAM 21.12. solver based on a multi-phase solver, multi-component incompressible solver based on a volume of fluid method is adapted to deal with diffusive-convective phase change. So as to reach this goal, an implementation of the enthalpy-porosity techinque is carried out. The work of Voller et al. is closely followed, and a detailed explanation of the used equations and the assumptions taken is given. Validation of the model is accomplished by comparing the results with the authors in Bourdillon and Kowaleski and Rebow.

On a second stage, a 2D semi-empirical model based on the work of Lee is adapted to account for the nucleation characteristics during the process of the water phase change. Validation of the model is done by comparing the obtained results to Neumann solutions for classical Stefan problem.

Finally, the current work is extended to couple a fluid region in which the liquid undergoes a phase-change and a solid region. This is done in the context of a conjugate heat transfer environment.

Keywords: PCMs, multip-phase, Enthalpy-porosity technique, Lee model, Stefan problem, conjugate heat transfer, OpenFOAM.

Acknowledgements

My first and biggest thanks goes to my supervisors, Dr. Robert Castilla and Dr. Gustavo Raush for their invaluable help throughout this work.
I would like to thank my family and all my workmates in Barcelona Technical Center S.L. for giving me support in the darkest hours.

Contents

List of Figures

List of Tables

Chapter 1

Introduction

1.1 Thesis Statement. Background and motivation

During the last decade, the use of phase change materials has been growing in the automotive industry.
These substances release or absorb large amounts of latent heat when they go through a change in their physical state, as the material reaches its specific phase change temperature. Thus, in the process of latent heat release or absorption, the temperature of the PCM remains constant. Therefore, PCMs are considered to be efficient in terms of thermal storage.

On the other hand, the use of these materials is not exclusive for thermal management. It is of relevant importance when used in conjunction with soap in the windshield wiper system of the car. In such zone, problems involving solidification are of considerable relevance. And this is mainly due to a volumetric expansion originated by the thermal effects within the PCM which at its turn, generates stresses in the polymeric tank in which is bottled up.

Therefore, this master's thesis main objective aims to study different numerical techniques to represent solidification process and, specially, pure water phase change. This is accomplished by first imlementing an enthalpy-porosity technique within the frame of a multi-phase incompressible solver based on volume-of-fluid (VOF) method for interface tracking. The objective of this first stage is to apply sensible and latent heat as source terms in the energy equation. On a second term, a 2D semi-empirical model based on the work of Lee is adapted to account for the nucleation characteristics occured during the water phase transition.

The final stage of this thesis is devoted to an implementation of a multiregion solver to calculate conjugate heat transfer problems between solid and fluid zones with the singularity of being, the fluid zone, capable of handling phase change materials.

The next chapters are mainly focused on describing phase-change phenomena and heat transfer mechanisms used along the completion of this master's thesis.

1.2 Phase-Change Process

The phase-change is usually modelled by a sudden change in enthalpy per unit of temperature generated within a narrow temperature range near the freezing point. Often, this process is assumed to behave in a characteristic temperature, as shown in Fig. **??**, leading to a moving boundary problem. However, at a given critical temperature, both fluid and solid phases may coexist giving a state called mushy region. In this case, one speaks of a non-linear diffusion problem rather than a moving boundary problem **krabbenhoft_damkilde_nazem_2006**.

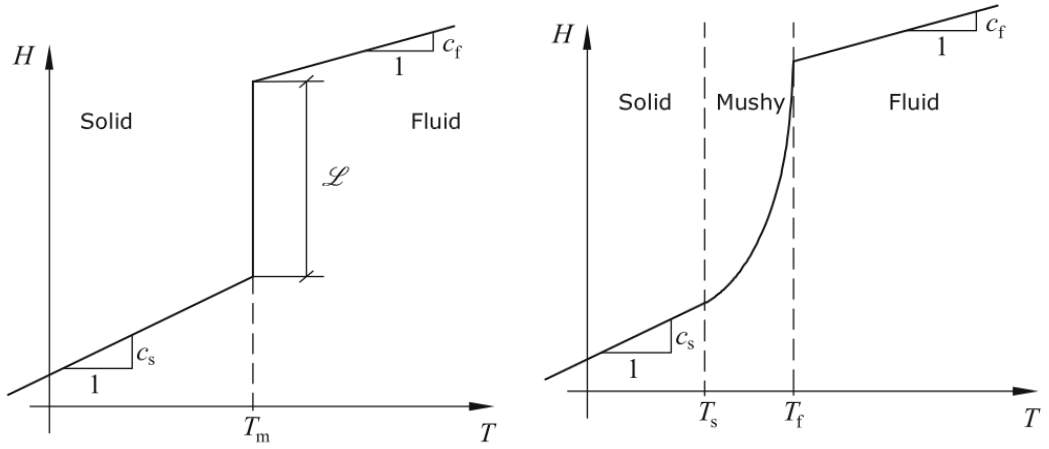

(A) Isothermal phase-change.

(B) Non-isothermal phase-change.

FIGURE 1.1: Phase-change comparison.

As briefly introduced, two types of phase-change are used to describe the way the latent heat is released or absorbed during freezing or melting processes:

- **Non-isothermal phase-change:** the phase-change takes place within a temperature range yielding a transition zone between a solid and a liquid phase called mushy zone. Typically, the thickness of this region is straightfully proportional to the temperature range in wich the phase-change occurs.
- **Isothermal phase-change:** the phase-change is arisen instantaneously at the melting temperature. The release or absorption of the latent heat occurs at this point in which, consequently, there is no transition zone between solid and liquid phases. At this point, there is a narrow line, mainly derived from the discretization of the computational domain, characterizing the phase-change phenomena.

As an important remark, when the mushy region is sufficiently narrow, the isothermal assumption is usually a good approximation. However, despite of the fact of being a convenient approach it may lead to significant complication when it comes to numerical solution techniques.
Along the next chapters, a more detailed description on existing techniques that deal with such non-trivial phenomena will be given.

1.2.1 Water phase-change

In a similar manner, the water phase-change takes place. A complex interaction of the molecular forces generate water to behave in a curious way when it gets frozen into ice. The vast majority of substances, when they are cooled, become more dense in the frozen state than when liquid. However, when cooled under a specific temperature, water begins to expand and, once it starts freezing, it becomes less dense than water.

1.2.2 Phase diagram of ice

Ice crystals undergo different kinds of structures. Called ice Ih, in the form of hexagonal ice and, manifested in six cornered snow flakes, is the natural ice found

in earth. However, at lower pressures below 2 kbar, many other ice structures may exist.
The ice phase diagram shown below, points out the conditions of stability for all ice phases. As it is cleared out, the line between the water and ice Ih is an equilibrium line with a negative slope, consequence of having, the solid, lower density than the liquid. These equilibrium lines extend in the form of metastable phase boundaries into the area of stability of other ice phases. Although there are at least 11 crystalline ice shapes, the only which is found in naturally on earth is the hexagonal form.
As a remark, the implication that there is a rise on the pressure would not propitiate ice formation at 0ºC, instead water would need to be cooled down.

1.2.3 Properties of ice

Ice, when subjected to visible light conditions, is transparent and has the lowest index of refraction for the sodium spectrum of any known crystalline material[].
Mechanically, ice behaves like a viscoelastic material with a non linear law. Polly-crystalline ice subjected to stress, deforms elastically, followed by a transient creep and finally, a secondary creep in the form of steady viscous flow is obtained.
As pointed out in [], the surface of ice Ih near the melting point has many dangling broken bounds that boost the presence of a liquid-like layer and as a consequence, low friction on such surface. Variation of density of ice with phase at 110 K and some physical properties of ice Ih at 0ºC are described in the tables below.

1.2.4 Freezing phenomena

Time-temperature diagram for freezing of pure water (ABCDE) and aqueous solutions (AB'C'D'E') show the physical process that occurs during the solidification. The first stage, from A to B, belongs to undercooling, also called supercooling, and it is arisen below the freezing point T_f, which is equal to the melting point, T_m. This point is referred to a non equilibrium point and it is analogous to an activation energy necessary for the nucleation process. Before nucleation process, pure water may need to be cooled down several degrees. At point B, the system nucleates and releases its latent heat faster than the heat which is being removed from itself.
From C to D, the horizontal axis shows the evolution of the crystal growth in time. At C, there exists the nucleation point and, from there through D, latent heat gets removed out of the system at constant temperature. In this way, the mixture, which is in a partially frozen state, does not cool until all the potentially freezable water has crystallized.

1.3 Mechanisms of Heat Transfer. Heat convection

The process of water freezing in enclosures is common in engineering. When there exist temperature gradients within the liquid phase in the process of solidification, a natural buoyancy driven flow is initiated and such behavior is determined to affect the shape of the liquid/solid interface as well as the progress of solidification. Indeed, these temperature differences in the liquid cause density variations so that the natural motion occurs. Boussinesq approximation can be validly used for fluids whose density varies linearly with temperature. However, pure water exhibits a maximum in its density when it ranges between 0ºC and 4ºC. Beyond this last

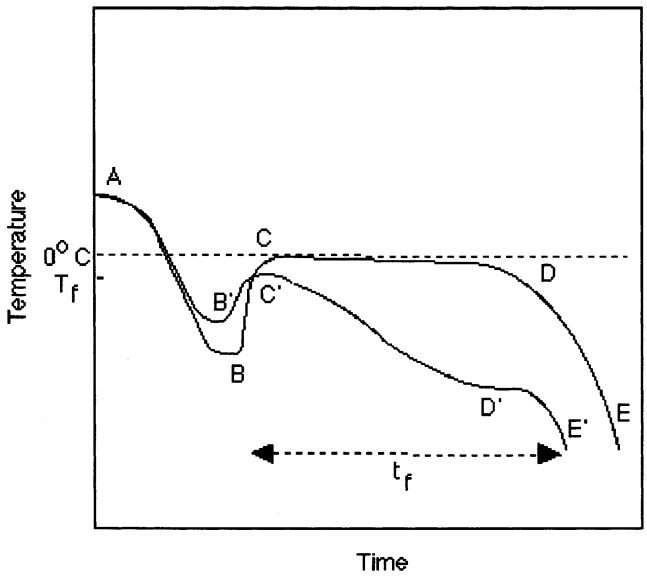

FIGURE 1.2: Process of crystallization of water.

temperature, and known as density inversion point, density decreases in a nonlinear manner as the temperature passes through the freezing point. In convective heat transfer, surroundings of the temperature where the aforementioned maximum happens to be, behave in a complex manner leading to fully control the process of growth of the solid phase.

1.4 Conjugate Heat Transfer. Heat conduction

Conjugate heat transfer is referred to the heat transfer between solids and fluids. Heat transfer in fluids is occurred mainly through a combination of two mechanisms: convection, due to a random motion of particles (diffusion) and advection, due to the bulk motion of the fluid. On the other hand, heat transfer in solids is mainly driven by conduction which accounts for the vibration and collision of the particles forming the solid.

Chapter 2

Numerical Methods for Phase-Change Phenomena

2.1 State of Art. Numerical Methods

Considering the PCM density as constant in the model might be thought as a reasonable assumption in some cases, in others where thermo-mechanical coupling between the fluid and its container is intended, it makes impossible to account for some physical behaviors which may result from expansion or contraction during the phase change of the material. However, the main goal of this thesis is not to present a method that represents thermo-mechanical coupling but a technique that ensures volume expansion due to density changes through the fluid domain. To reach this point, it is important to point some of the numerous researches that have been conducted in order to investigate the problem of solidification and melting.

At the present, the main numerical methods representing the treatment of liquid-solid phase change are divided into these categories:

- Surface tracking methods,
- Volume tracking methods,
- Moving mesh methods,

Surface tracking methods

Volume tracking methods

Moving mesh methods

2.2 Solidification methods

The challenge of a numerical investigation of a solidification process is to capture the free surface for the flow of the phase change material and, at the same time, account for the moving boundary induced by the phase change within the PCM. The free surface may be handled by the volume-of-fluid (VOF), originally introduced by [ref Hirt]. VOF relies on the definition of a transport indicator function within the finite volume method's framework. Simultaneously, and in order to account for the phase changes, some of the used models are based on meso-scale. This is the phenomena occurring between microscopic and continuum length scales and, in the current context, the complex micro structure generated during the solidification is approximated as liquid, mushy (intermediate state), and solid regions. Mushy region is thereby described as an averaged value of the liquid and solid properties.

One of the most used methods is the enthalpy-porosity technique, originally developed by Voller and Prakash [ref. Voller], which uses the typical conservation equations on a fixed Eulerian grid. The main concepts underlaying such method are: on the one side, an additional source term to the energy conservation equation is applied to describe the release of latent heat. On the other side, the solidification effects on the mass transport are modelled as a porosity variable and this is introduced as a Darcy-type source term to the momentum equation.

Some of the studies found on this topic, the coupling of both VOF and enthalpy-porosity methods are mainly related to casting processes. Rösler and Brüggermann [ref] introduced a numerical model for a solid-liquid phase change inside a latent heat thermal energy storage. Richter et al. [ref] worked out a method for the simultaneous moult filling and solidification process which settles the developing of free surface flow and the liquid-solid phase transition under the volume-of-fluid and enthalpy-porosity methods. However, no adaptation of these methods to purely solidification processes has been found. Therefore, and, the objectives of this research are:

- To introduce a new solver based on the coupling of VOF and enthalpy-porosity techniques which covers the relevant physical effects during the process of solidification.
- To validate simulation results by using benchmark cases found in the literature.

Numerical methods commented are briefly described next.

On the other hand, semi-empirical methods ...

2.2.1 Volume-of-Fluid Method: General Aspects

The volume of fluid method takes relevance when fluids coexist with other phases. An example could be the ice (solid phase) advancing front within the liquid phase. The surface in between both phases needs to be solved by means of the volume of fluid technique.
This is sometimes seen as the conservation of the mixture components along the path of a fluid region. The equation which allows that is described as:

$$\frac{\partial \gamma_{\text{phase}}}{\partial t} + \frac{\partial \left(\gamma_{\text{phase}}\, u_j\right)}{\partial x_j} = 0 \tag{2.1}$$

In which α_{phase} corresponds to the phase fraction and it applies

$$\gamma_{phase} = \begin{cases} 0 & = \text{ solid PCM} \\ 0 < \gamma_{phase} < 1 & = \text{ cell contains the interface} \\ 1 & = \text{ liquid PCM} \end{cases} \tag{2.2}$$

2.2.2 Enthalpy-Porosity Model. Governing Equations

The energy equation based on the enthalpy formulation for convective-diffusive heat transfer states that,

$$\frac{\partial \rho h}{\partial t} + \frac{\partial}{\partial x_j}\left(\rho u_j h\right) = \frac{\partial}{\partial x_j}\left(\lambda \frac{\partial}{\partial x_j} T\right) \tag{2.3}$$

where u is the velocity component and λ is the thermal conductivity of the fluid. h can be expressed as a function of its latent heat and the specific sensible parts, However, the enthalpy-porosity method describes the enthalpy h of the mixture by its sensible part and the latent heat of solidification. The release of the latent heat is dependent on the stage of the phase change, and must be restricted to the phase change material.

$$h = \int_{T_r}^{T} c_p dT + \alpha_\ell L \tag{2.4}$$

where the latent heat is is driven by the evolution of the liquid α_l. The phase transition is modelled by expressing the liquid volume fraction as a function of the temperature,

$$\alpha_l = \begin{cases} 1 & T > T_{liq} \\ \frac{T - T_{\text{sol}}}{T_{\text{liq}} - T_{\text{sol}} + \varepsilon} & T_{\text{sol}} < T < T_{liq} \\ 0 & T < T_{\text{sol}} \end{cases} \tag{2.5}$$

For seek of brevity on the following expressions, it is adapted the term γ_{phase} to γ_l If expression 2.4 is replaced in 2.3,

$$\begin{aligned} &\frac{\partial \left(\rho c_p T + \gamma_l \alpha_l L\right)}{\partial t} + \frac{\partial \left(\rho u_j c_p T + u_j \gamma_l \alpha_l L\right)}{\partial x_j} \\ &= \frac{\partial}{\partial x_j}\left(\lambda \frac{\partial T}{\partial x_j}\right) \end{aligned} \tag{2.6}$$

Rearranging terms, it yields,

$$\begin{aligned} \frac{\partial(\rho C_p T)}{\partial t} + \frac{\partial(u_j \rho C_p T)}{\partial x_j} + L\left[\frac{\partial(\rho \alpha_l \gamma_l)}{\partial t} + \frac{\partial(u_j \rho \alpha_l \gamma_l)}{\partial x_j}\right] &= \frac{\partial}{\partial x_j}\left(\lambda \frac{\partial T}{\partial x_j}\right) \\ S = -L\left[\frac{\partial(\rho \alpha_l \gamma_l)}{\partial t} + \frac{\partial(u_j \rho \alpha_l \gamma_l)}{\partial x_j}\right] & \end{aligned} \tag{2.7}$$

The momentum equation is discussed in detail in the sub-chapter *Interphase porosity models*.

2.2.3 Lee model

The Lee model is based in the liquid-vapour mass transfer. Governed by the vapour transport equation 2.8, this model is applicable during melting or solidification of a fluid.

$$\frac{\partial}{\partial t}\left(\alpha_i \rho_i\right) + \nabla\left(\alpha_i \rho_i u_i\right) = S_{m_i} \tag{2.8}$$

ρ_i and u_i are the fluid density and fluid velocity of the *ith* phase. Moreover, S_{m_i} is the mass source which takes on a zero value at the interface.
During melting, $T_l > T_{sat}$,

$$\frac{dm_{sl}}{dt} = C_f \rho_s \alpha_s \left(\frac{T_s - T_{sat}}{T_{sat}}\right) \tag{2.9}$$

During solidification, $T_l < T_s at$

$$\frac{dm_{ls}}{dt} = C_f \rho_l \alpha_l \left(\frac{T_{sat} - T_l}{T_{sat}}\right) \tag{2.10}$$

The coefficient C_f might be interpreted as a time rate and must be empirically tunned. Its magnitude is expressed in $\frac{1}{s}$. α represents the phase volume fraction. $\frac{dm_i}{dt}$ are the mass transfer rates from one phase to another. The subscripts *"s"*, *"l"*, refer to solid and liquid phases respectively. T_{sat}, is the phase transition temperature which, in case of pure water would be 273.15 K. The source term of 2.8 is then calculated as,

$$S_{m_i} = \begin{cases} \frac{dm_{sl}}{dt} - \frac{dm_{ls}}{dt}, & \text{for water phase} \\ \frac{dm_{ls}}{dt} - \frac{dm_{sl}}{dt}, & \text{for ice phase} \end{cases} \tag{2.11}$$

2.2.3.1 Momentum Equation

In the momentum equation, the flow is modelled as,

$$\begin{aligned} &\frac{\partial\left(\rho u_i\right)}{\partial t} + \frac{\partial\left(\rho u_i u_j\right)}{\partial x_j} \\ &\quad = -\alpha_i \nabla p + \frac{\partial}{\partial x_j}\left(\mu \frac{\partial u_i}{\partial x_j}\right) + F_{\sigma i} + S_{u_i} \end{aligned} \tag{2.12}$$

The source term for the momentum equation can be written as,

$$S_{u_i} = \begin{cases} \frac{dm_{sl}}{dt} u_l - \frac{dm_{ls}}{dt} u_s, & \text{for water phase} \\ \frac{dm_{ls}}{dt} u_s - \frac{dm_{sl}}{dt} u_l, & \text{for ice phase} \end{cases} \tag{2.13}$$

where u_l and u_s are the liquid and solid velocity components accordingly.
The source terms related to interphase porosity (2.29) may be added to the momentum equation presented here for the Lee model 3.6.

2.2.3.2 Energy Equation

The energy equation for the Lee model can be described as,

$$\frac{\partial(\rho C_p T)}{\partial t} + \nabla \cdot \left(u_j \rho C_p T\right) = \nabla \cdot \left(k_i \nabla T_i\right) + S_{H_i} \tag{2.14}$$

where the heat source term due to mass transfer in the energy equation is calculated as,

$$S_{h_i} = \begin{cases} \frac{dm_{sl}}{dt} H_L, & \text{for water phase} \\ \frac{dm_{ls}}{dt} H_L & \text{for ice phase} \end{cases} \tag{2.15}$$

where H_l is the latent heat induced by the phase transition and k_i, the thermal conductivity.

2.2.3.3 Classical nucleation theory. The coefficient C_f.

The coefficient C_f that appears on Equations 3.2 and 3.3 is computed accordingly to the work of Huang, Wang, and Li, 2020. In these work, the Lee model is used and the nucleation rate is introduced for the calculation of mass transfer rate between phases.
The concept behind the *Classical Nucleation Theory*, CNT, as described in Ickes et al., 2015 resides in the idea of droplet freezing. This is initiated in the fluctuation of molecules of a supercooled liquid due to thermal vibration which lead, at its turn, to spontaneous formation of ordered solid molecule clusters (ice embryos). The size of

these embryos oscillates as individual water molecules are crystallized or lost from the liquid phase. When the size of the embryo reaches a critical value, it leads a faster and auspicious thermodynamic joining of further water molecules to the crystal lattice. This means the critical embryo enhancing the "parent phase", supercooled liquid, to undergo a macroscopic phase transition: droplet freezing.
And this is what CNT aims to describe; the freezing process in terms of temperature-dependent nucleation rate by joining two components: thermodynamic and kinetic. These components, briefly described in the following chapters, are based on the theory found at Wu, Lai, and Zhang, 2015 and Huang, Wang, and Li, 2020, and adapted in Huang, Wang, and Li, 2020.
As a remark, in this thesis a brief introduction of this theory is given. However, for further details on the assumptions used refer to the literature.

Thermodynamic component

This thermodynamic component seeks for the number of critical embryos formed per unit of volume at a specific temperature. A decrease in the enthalpy, and consequently a change in Gibbs free energy required to form an ice embryo containing water molecules generates an energy barrier to nucleation. However, for ice embryo formation, this barrier needs to be overcome.

$$\Delta G_C = \underbrace{\Delta G_V}_{\text{volume term}} + \underbrace{\Delta G_S}_{\text{surface term}} \tag{2.16}$$

$$\Delta G_c = -\frac{4}{3} \cdot \frac{\pi r^3}{\Omega} \cdot \Delta g_v + 4\pi r^2 \gamma_{sf} \tag{2.17}$$

where r is the radius of a simplified spherical embryo, γ_{sf} the interfacial tension between phases Ω the volume of a single molecule ($\Omega = V_{m,w}/N_A$), $V_{m,w}$ is the molar volume and Δg_v represents the decrease in volume of the Gibbs free energy of a molecule and is defined as:

$$\Delta g_v = \frac{\Delta_m H_1}{N_A} \frac{\Delta T}{T^*} \tag{2.18}$$

where $\Delta_m H_1$ is the molar latent heat of crystallization, N_A is the Avogadro's number, T^* is the freezing temperature and $\delta T = T^* - T$, the degree of supercooling. The radius has an influence on the change in Gibbs free energy. This is when:

- $r < r_{crit} \Rightarrow \Delta G_c > 0 \;\; || \;\; \Delta G_c \uparrow \;\; \Rightarrow \;\; r \uparrow \Leftarrow$ endothermic process
- $r > r_{crit} \Rightarrow \Delta G_c < 0 \;\; || \;\; \Delta G_c \downarrow \;\; \Rightarrow \;\; r \uparrow \Leftarrow$ exothermic process

The critical radius exists when the global enthalpy variation gets negative.
By differentiating Eq. 3.11 and setting $\frac{d(\Delta G_c)}{dr} = 0$, the critical radius is defined as:

$$r_{crit} = \frac{2\gamma_{sf} T^* V_{m,w}}{\Delta_m H_1 \Delta T} \tag{2.19}$$

Then, if subsituting Eq. 3.12 and 3.13 in Eq. 3.11, it is obtained the energy barrier:

$$\Delta G_{crit} = \frac{16\pi}{3} \cdot \frac{\gamma_{sf}^3 V_{m,w}^2 T^2}{\Delta_m H_1^2 \Delta T^2} = \frac{1}{3} \left(4\pi r_{crit}^2 \gamma_{sf}\right) \tag{2.20}$$

In Huang, Wang, and Li, 2020, the expression concerning the variation of Gibbs function for the phase change does not include the molar volume of water but a

shape coefficient of nucleation. It involves the influence of the contact angle when going from a uniform state to an inhomogeneous. This shape factor is defined as:

$$\alpha_{ey} = \frac{2 - 3\cos\theta + \cos\theta^3}{4} \tag{2.21}$$

Temperature and saturation dependent number of ice embryos per unit volume of water may be expressed in a Boltzmann distribution form using ΔG:

$$N_{\text{embryo}}\left[\text{m}^{-3}\right] = N_{\text{l}} \cdot \exp\left(-\frac{\Delta G}{k_{\text{B}} T}\right) \tag{2.22}$$

where N_1 is a volume-based number density of water molecules in the liquid phase.

Kinetic component

The kinetic part of the nucleation rate is introduced in the form of water molecules flux. This is expressed as a Boltzmann distribution such that:

$$\Phi = \frac{k_B T}{h} \cdot \exp\left(-\frac{\Delta g}{k_{\text{B}} T}\right) \tag{2.23}$$

where h is the Planck's physical constant, and Δg the activation energy for the transfer of a water molecule across the phase boundary.
The rate at which the water molecules are transferred into an ince embryo is defined as:

$$K = n_{\text{s}} \cdot 4\pi r_{\text{embryo}}^2 \cdot Z \cdot \Phi \tag{2.24}$$

where n_s is the number of molecules and $4\pi r_{\text{embryo}}^2$ is the surface area of the critical embryo and Z a kinetic prefactor. For seek of simplification, the authors of the theory suggest that the product of these terms are close to unity. Thus, considering this change, the equation yields as:

$$K = \Phi \tag{2.25}$$

Nucleation rate

Combining the thermodynamic component Eq. 3.15 and the kinetic one 2.25, the formulation of the nucleation rate can be expressed as:

$$J_{\text{hom}}\left[\text{m}^{-3} \cdot \text{s}^{-1}\right] = \underbrace{K}_{\text{Kinetics}} \cdot \underbrace{N_{\text{l}} \cdot \exp\left(-\frac{\Delta G}{k_{\text{B}} T}\right)}_{\text{Number of embryos}} \tag{2.26}$$

As a final step, inserting Eq. 3.18 into Eq. 3.19, the nucleation rate is expressed in the form of:

$$J_{\text{hom}}\left[\text{m}^{-3} \cdot \text{s}^{-1}\right] = \frac{k_B T}{h} \cdot \underbrace{\exp\left(-\frac{\Delta g^{\#}}{k_{\text{B}} T}\right)}_{\text{diffusion of molecules effect}} \cdot N_1 \cdot \underbrace{\exp\left(-\frac{\Delta G}{k_{\text{B}} T}\right)}_{\text{nucleation effect}} \tag{2.27}$$

Fig. 2.1 characterizes the variation of the crystallization rate in function of the temperature. In the image, the dotted line shows how the nucleation effect is 0 close to the cooling, and as the temperature values decrease, this lines tend to 1. Moreover, the dashed line shows how the effect of the diffusion of the molecules increases as the temperature does. This prompts out the ease of the embryo formation when at low temperatures since the molecules cannot overcome the energy barrier to enter the embryo. However, the crystal growth becomes harder. This may be seen as constant search of equilibrium among the nucleation and the crystal growth. Finally, the

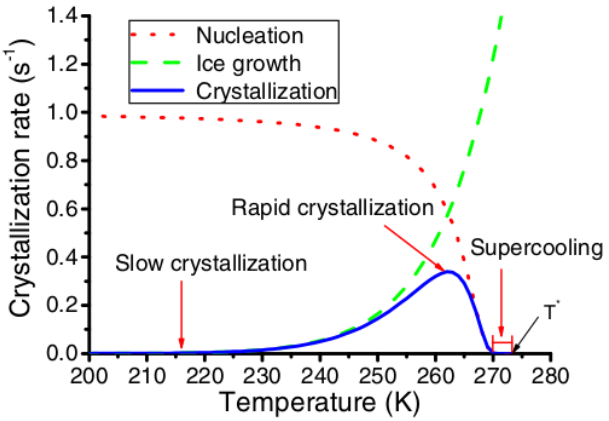

FIGURE 2.1: Crystallization rate versus temperature.

coefficient C_f that appears on Equations 3.2 and 3.3 as commented above, is defined for the Lee model as:

$$C_f = J_{\text{hom}} \cdot V_l \tag{2.28}$$

where V_l is the volume of water in each cell.

2.2.4 Interphase porosity models

Interphase porosity models add an aritificial momentum source over the interface between phases to compute the sink of velocity in the solidified region. Therefore, influencing the behavior of the physics during the process of solidification or melting.
The model implemented in OpenFOAM is *Voller Prakash method* and it defines the source terms, S_y and S_z such that when along the fluid domain these terms take on a value of zero, the momentum equations are driven by the actual values of the velocities. On the other side, when it comes to treat the mushy region (i.e. porous region), the value of these source terms dominate convective, diffusive and transient terms and the momentum equation tends to approximate de Darcy law.
The two source terms as specified above,

$$\begin{cases} S_y = -Av \\ S_z = -Aw \end{cases} \tag{2.29}$$

Then, to specify a term for the function A, it is used the *Carman-Koseny equation*, which is derived from the Darcy law. The former expresses the gradient for the pressure as a combination of the velocity, $\mathbf{u}$, and the porosity, λ. The coefficient C

depends on the morphology of the medium.

$$gradP = -\left(\frac{C(1-\lambda)^2}{\lambda^3}\right)\mathbf{u} \tag{2.30}$$

To avoid division by zero, q is added to the equations shown

$$A = -\left(\frac{C(1-\lambda)^2}{\lambda^3+q}\right) \tag{2.31}$$

The source terms S_y and S_z are added in the Eq. 3.33 and 3.34. The source term S_b corresponds to the body forces of the fluid and will be discused later on this thesis.

$$\frac{\partial(\rho v)}{\partial t} + \mathrm{div}(\rho\mathbf{u}v) = \mathrm{div}(\mu\,\mathrm{grad}\,v) - \frac{\partial P}{\partial y} + S_y \tag{2.32}$$

$$\frac{\partial(\rho w)}{\partial t} + \mathrm{div}(\rho\mathbf{u}w) = \mathrm{div}(\mu\,\mathrm{grad}\,w) - \frac{\partial P}{\partial z} + S_z + S_b \tag{2.33}$$

2.2.4.1 Surface tension model

The surface tension is only specified on a phase pair basis. In this version of OpenFOAM, it is present a constant model for a given σ.

Chapter 3

Numerical Simulation of Solidification Process

3.1 OpenFOAM. General Aspects

OpenFOAM is a free open-source software written in C++ and mainly conceived to perform computational fluid dynamics (CFD) simulations based on a finite volume discretization (FVM).

3.1.1 The finite volume method

Fluid equations usually take the form of non-linear partial differential equations and so, most of time, no analytical solution can be derived from them. In that context, different numerical techniques are employed to reach an approximation of the solution to these problems. These methods require a discretization of the domain in which the solution is going to be calculated. As aforementioned, OpenFOAM uses the finite volume method, which is, indeed, one of the most widely techniques used in computational fluid dynamics, and the one used in this thesis.
This technique turns the partial differential equations, which at their turn represent conservation laws over differential volumes, into discrete algebraic equations over finite volumes. Similarly to the finite element method, the FVM also needs a discretization of the geometric domain but in this numerical method, the elements used to integrate the algebraic equations representing the conservation partial differential equations are finite volumes or non-overlapping elements.
Some of the terms in the conservation equation are converted into face fluxes and evaluated in the discretized finite volumes. These face fluxes are strictly conservative. This is that the flux entering the volume is equal to the flux leaving the adjacent volume. This property makes the finite volume method the preferred technique for CFD **moukalled_mangani_darwish_2016**.

Geometric domain discretization

The intrinsic properties of the finite volume method need the computational domain to be discretized in volume cells, known as control volumes (CV). Each one of these volumes has a centroid or computational point in which the solution is obtained. Alongside with this idea, OpenFOAM follows a cell-centered approach in which the unknowns are defined at the center of these volumes or cells. The value of these are computed as an average value of the variable in that cell.
Moreover, the control volume is defined by the neighbours. This is, in the case the volume has an adjacent neighbour, an internal face is delimiting the separation of

both. On the other hand, if the volume is not sharing a face with a neighour volume, the face is considered to be a boundary.

Fluid dynamic equations discretization

The continuity equation, the Navier-Stokes equations and, the heat equation stated in section 2 can be stated in a more general form under the formulation of the Reynolds transport theorem:

$$\underbrace{\int_{V_P} \frac{\partial \rho\phi}{\partial t} dV}_{\text{Temporal term}} + \underbrace{\int_{V_P} \nabla \cdot (\rho \vec{u}\phi) dV}_{\text{Convective term}} = \underbrace{\int_{V_P} \nabla \cdot \left(\rho \Gamma_\phi \nabla \phi\right) dV}_{\text{Diffusive term}} + \underbrace{\int_{V_P} S_\phi dV}_{\text{Source term}} \tag{3.1}$$

where V_P is the control volume cell, ϕ may be any scalar or vectorial variable of the continuum, Γ_ϕ is the diffusivity of the variable and S_ϕ is a source term.
The fluid variable is defined as a ratio of itself integrated along the volume cell. Thus, it yelds the following form,

$$\phi = \phi_P = \frac{1}{V_p} \int_{V_P} \phi(x) dV \tag{3.2}$$

Therefore, a complete discretization of the previous terms is needed to solve the physics regarding a general fluid dynamics problem.

3.1.2 OpenFOAM functioning

In this first section, a brief introduction on the structure and functioning of the OpenFOAM software is given. In the folder structure tree shown in Fig. **??**, it is shown a typical case setup for a phase change problem using *icoReactingMultiphaseFoam* solver.

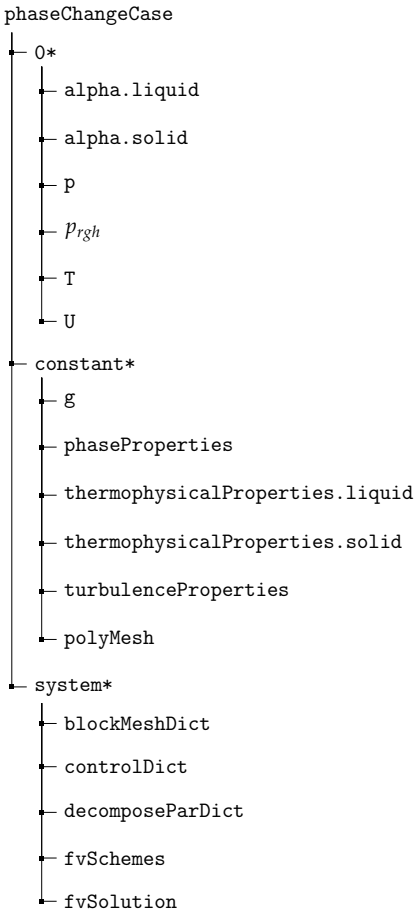

FIGURE 3.1: General structure of an OpenFOAM case.

3.1.3 Boundary Conditions Directory

The "0" directory gathers all the boundary conditions at time zero and the initial conditions to set up the case. As the simulation starts running, the information of these fields is saved in folders at every timestep.

3.1.4 Constant Properties Directory

The "constant" directory contains all the information typically regarding the physical properties which are kept constant through the simulation. Moreover, once the dictionary *blockMeshDict* is run, OpenFOAM creates a folder called *polyMesh* containing all the information relevant to the mesh (points, faces,...)

3.1.5 System Directory

This folder contains the files required by the control of the solver and the solution itself. The most common files are:

- **blockMeshDict:** in this file the parameters required to build up the computational domain, the mesh and the boundaries are found. The command **blockMesh** executes this dictionary creating the *polyMesh* folder commented above.

- **controlDict:** Time parameters associated to the computation are set in this file.
- **decomposeParDict:** In the realization of this thesis, the help of parallel computing is required. Thus, in this file, parameters regarding the decomposition of the mesh are configured. It is executed by means of the **decomposePar** appliation implicit in OF. The mesh is afterwards reconstructed by using **reconstructPar**
- **fvSchemes:** Schemes selected for the discretization of the derivative terms are defined. Among others, time schemes, gradient schemes, laplacian schemes, divergent schemes, interpolation schemes can be declared here.
- **fvSolution:** contains sub-dictionaries used to control the solvers and the solution algorithms. It also allows the definition of the fields resolution.

3.2 Solidification process. Methodology

A convection solver is used to represent the flow behavior generated by the density difference due to existing temperature gradients whithin the volume of control. A polynomic water density is implemented in the native OpenFOAM solver and compared with the standard Boussinesq approximation. The current model is validated against numerical results form the literature. The solution of this convection solver is later used as a boundary condition, before solidification phenomena plays a role.

3.3 OpenFOAM: BuoyantBoussinesqPimpleFOAM. Natural Convection solver

In a natural convection environment, the motion of the fluid is mainly driven by the density difference within the fluid volume of control. At its turn, the differences in the density, responsible for buoyancy forces, are generated by the existing temperature gradients. Within a physical context, the fluid near a hot heat source gets warmed up and, as a result, it becomes less dense moving up inside a domain. Consequently, the fluid in contact of the cold heat source is pushed from its zone to replace the hot fluid location. At this point, the cycle starts again repeating the phyisical phenomena.

3.3.1 Case Description

Within the context of natural convection, the current case aims to develop a comprehensive state of the capabilities that OpenFoam solvers brings to solve this phenomena. To reach the objective, and on purpose of controlling the physics generated on the simulation, a regular squared geometry of 0.038 *mm* side length is created:

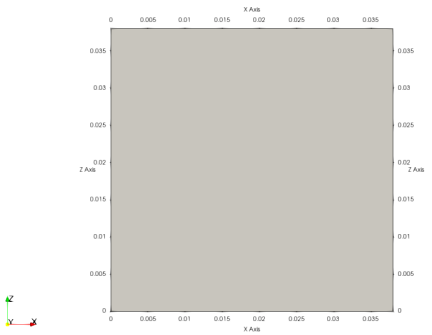

FIGURE 3.2: Geometry of the case.

3.3.2 Hypotheses And Assumptions

To carry out the problem-being, a series of assumptions are taken into account in order to simplify the solving of the fluid equations involved.
Laminar regime: The Reynolds number, computed from the maximum velocity is not high enough to consider turbulent effects.
Convective heat transfer: To determine whether the heat transfer is assumed to be convective, the Prandtl number and the Rayleigh number should be assessed.
The Prandtl number, as the relation between the viscosity and the thermal conductivity of a fluid or, in other words, the correlation between momentum transport and thermal transport capacity is calculated as:

$$\mathrm{Pr} = \frac{v}{\alpha} = \frac{\eta}{\rho\alpha} = \frac{\eta c_p}{\lambda} = \frac{\text{momentum transport}}{\text{heat transport}} \tag{3.3}$$

where Thus, a small Prandtl number are owned by free-flowing flows with high thermal conductivitiy.
On the other hand, the Rayleigh number is referred to the time scale relation between

the diffusive and the convective thermal transports. It is thus used to determine wheter the buoyancy-driven natural convection plays an important role in the heat transfer. The dimensionless number is assessed in this context by this form:

$$\mathrm{Ra}_x = \frac{g \cdot \beta}{\nu \cdot \alpha} \cdot (T_s - T_{\mathrm{inf}}) \cdot x^3 \tag{3.4}$$

Being g, the gravity, β, the coefficient of thermal expansion, ν, the kinematic viscosity, α, the thermal diffusivity, and T_s and T_{inf}, the temperature on the wall surface and the temperature of the fluid far from the wall accordingly.
In the current case-scenario, a Prandtl close to 7 and a Rayleigh of 2517629 determine a convective heat transfer.
Newtonian fluid: The viscosity of the fluid is assumed to be constant.
Thermophysical properties: specific heat, C_p, the thermal expansion coefficient, β, thermal conductivity, κ, kinematic viscosity, ν are assumed to be non-dependent of temperature. However, the density will be dependent of temperature so as it plays an important role in the buoyancy effects through the later explained in this section.

The conservative equations used to describe the motion of the fluid along time and space are described next.

3.3.3 Governing Equations

In this section, the governing equations for the used solver are described first. The conservation of mass states that the mass flowing into the volume of control (CV) must be equal to the mass flowing out of such volume.

$$\frac{\partial v}{\partial y} + \frac{\partial w}{\partial z} = 0 \tag{3.5}$$

3.3.3.1 Momentum Equation

Throughout the CV the momentum of the fluid flow is preserved and here below it is expressed for the y-direction and z-direction.

$$\frac{\partial(\rho v)}{\partial t} + \mathrm{div}(\rho \mathbf{u} v) = \mathrm{div}(\mu\, \mathrm{grad}\, v) - \frac{\partial P}{\partial y} \tag{3.6}$$

$$\frac{\partial(\rho w)}{\partial t} + \mathrm{div}(\rho \mathbf{u} w) = \mathrm{div}(\mu\, \mathrm{grad}\, w) - \frac{\partial P}{\partial z} + S_b \tag{3.7}$$

where in the case of the *Boussinesq approximation* where the density variation is linear:

$$S_b = g \cdot \rho_r [1 - \beta(T - T_r)] \tag{3.8}$$

in the case of the implemented polynomial density which accounts for the inversion point as in Bourdillon, 2016:

$$S_b = g \cdot [\rho_r - \rho(T)] \tag{3.9}$$

where the polynomial expression from ρ is:

$$\begin{aligned} \rho(T) = {} & 999.840281167108 + 0.0673268037314653 \times T \\ & - 0.00894484552601798 \times T^2 \\ & + 8.78462866500416.10^{-5} \times T^3 - 6.62139792627547.10^{-7} \times T^4 \end{aligned} \tag{3.10}$$

As it will be pointed out later, the native solver uses the Boussinesq approximation to account for the buoyancy effects. However, this linear assumption is only valid as the density variations meet:

$$\frac{\Delta\rho}{\rho_r} << 1 \tag{3.11}$$

Therefore, to account for the inversion points present during the freezing process, a density variation like the described in **??** is implemented in the solver.

3.3.3.2 Temperature Equation

The temperature equation representing the convection phenomena yields as:

$$\frac{\partial T}{\partial t} + \frac{\partial (u_j T)}{\partial x_j} = \frac{\partial}{\partial x_j}\left(\gamma \frac{\partial T}{\partial x_j}\right) \tag{3.12}$$

where the thermal diffusivity, γ, is defined as:

$$\gamma = \frac{\lambda}{\rho_r c_p} \tag{3.13}$$

All these equations are regarded by the solver *buoyantBoussinesqPimpleFoam*.

3.3.4 Solver descripton. Control Loop

The *buoyantBoussinesqPimpleFoam* is a solver used to solve non-steady buoyancy-driven fluids by using the Boussinesq approximation as a coupling between density and temperature fields. It considers the fluid as incompressible and uses the PIMPLE algorithm for the pressure-velocity coupling. The flowchart of the integration procedure for the presented solvers *buoyantBoussinesqPimpleFoam* and *icoReactingMultiphaseinterFoam* is presented below:

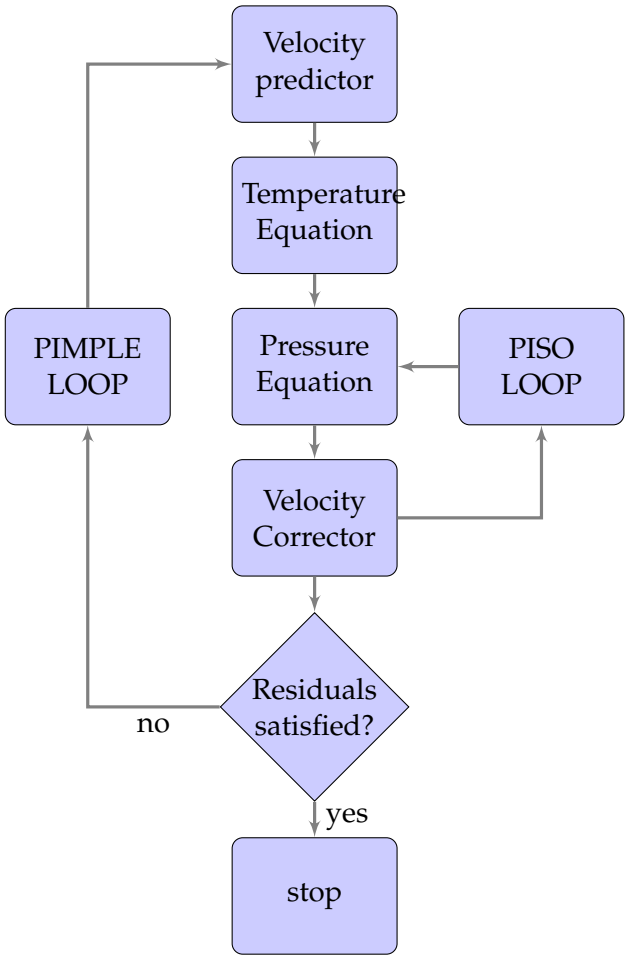

FIGURE 3.3: Flowchart of integration procedure. *buoyantBoussinesqPimpleFoam*

3.3.5 Code implementations

As described in the *Governing equations* section, the need for a polynomial density expression and a variation of the momentum source terms devoted to reflect the buoyancy effects is derived. To do so, a new equation of state is implemented within the OpenFoam framework. Now and, in order to take into account this bouyancy forces, the pressure equation is studied. This is beacause in the context of a pressure-velocity corrector scheme, and in the case of ensuring stability and simplifying the boundary conditions definition, the modified pressure, p_{rgh}, within the pressure equation implementation, is the term that accounts for the gravity terms.
Here, it is presented a general form of a momentum equation with the continuity equation corresponding to a incompressible flow.

$$\begin{cases} \frac{\partial(\rho \mathbf{v})}{\partial t} + \nabla \cdot (\rho \mathbf{v} \otimes \mathbf{v}) = -\nabla p + \nabla \cdot (\mu(\nabla \mathbf{v} + \nabla \mathbf{v}^T)) \\ \nabla \cdot \mathbf{v} = 0 \end{cases} \tag{3.14}$$

From this general equation, it will be given the term $H(\mathbf{u})$, as later on will be needed for the pressure equation calculation.
Therefore, this term comes from considering the linearization of the advective term

under the assumption of small Courant numbers (Co < 1). Leading the term $\mathbf{v}^0 \cong \mathbf{v}$.

$$\begin{aligned}\int_\Omega \nabla \cdot \left(\mathbf{v} \otimes \mathbf{v}^0\right) d\Omega &\cong \sum_f \mathbf{v}_f \mathbf{v}_f^0 \cdot \mathbf{S}_f \\ &= \sum_f F^0 \mathbf{v}_f \\ &= a_P \mathbf{v} + \sum_f a_N \mathbf{v}_N\end{aligned} \tag{3.15}$$

$$a_P \mathbf{v}_P = \mathbf{H}(\mathbf{v}) - \nabla p \tag{3.16}$$

$$\mathbf{H}(\mathbf{v}) = \underbrace{-\sum_f a_N \mathbf{v}_N}_{\text{Diagonal term}} + \underbrace{\frac{\mathbf{v}^0}{\Delta t}}_{\text{Off-diagonal term}} \tag{3.17}$$

where $\mathbf{v}^0$ is the velocity at previous time-step and F^0 is the face flux at the previous time-step.
In addition, by discretizing the continuity equation, it is possible to get the final form of the pressure equation.
So as to give stability to the solution and to simplify the boundary conditions definition **berberovic_van hinsberg_jakirlic_roisman_tropea_2009**, a modified pressure is defined as,

$$p_{rgh} = p - \rho_r \mathbf{g} \cdot \mathbf{x} + \rho(T) \mathbf{g} \cdot \mathbf{x} \tag{3.18}$$

being, the pressure gradient the next expression,

$$-\nabla p + \rho_r \mathbf{g} = -\nabla p_{rgh} - \mathbf{g} \cdot \mathbf{x} \nabla \rho_r + \mathbf{g} \cdot \mathbf{x} \nabla \rho(T) + \rho(T) \mathbf{g} \tag{3.19}$$

and rearranging terms,

$$-\nabla p + \rho_r \mathbf{g} + \mathbf{g} \cdot \mathbf{x} \nabla \rho_r - \mathbf{g} \cdot \mathbf{x} \nabla \rho(T) - \rho(T) \mathbf{g} = -\nabla p_{rgh} \tag{3.20}$$

If one tries to describe the discretized pressure equation in *buoyantBoussinesqPimpleFoam*, there is a first term called **phig**, which is,

$$\Phi_f^{\nu+1} = \Phi_u^{\nu+1} - \left[(\mathbf{g} \cdot \mathbf{x})_f \left(\nabla {\rho_r}^{n+1} \right)_f + (\mathbf{g} \cdot \mathbf{x})_f \left(\nabla \rho(T)^{n+1} \right)_f \right] \frac{\left| \mathbf{S}_f \right|}{(a_P)_f} \tag{3.21}$$

A face flux calculated by the term **H(v)**, appearing in equation **??**

$$\Phi_u^{\nu+1} = \Phi_f^{\nu+1} + \left(\frac{H\left(\mathbf{v}^\nu\right)}{a_P} \right)_f \cdot \mathbf{S}_f + \left(\frac{1}{a_P} \right)_f \mathrm{ddt\,PhiCorr}\left(\mathbf{v}^\nu, \Phi^\nu\right) \tag{3.22}$$

where ddt PhiCorr is a flux adjustment due to the time-step. This is resolved by applying a *Rhie-Chow interpolation*, **rhie_chow_1983**, the next term in the pressure equation, **phiHbyA**, reads as,

$$\Phi_f^{\nu+1} = \Phi_f^{\nu+1} - \left[\left(\frac{1}{a_P} \right)_f \left(\vec{\nabla} p_{rgh} \right)_f \right] \cdot \mathbf{S}_f \tag{3.23}$$

The p_{rgh} term is thus assembled as,

$$\sum_f \left[\left(\frac{1}{a_P} \right)_f \left(\vec{\nabla} p_{rgh}^{\nu+1} \right)_f \right] \cdot \vec{S}_f = \sum_f \Phi^{\nu+1} \tag{3.24}$$

The flux, ϕ, is adjusted by the p_{rgh} term yielding the following expression,

$$\Phi_f^{\nu+1} = \Phi_f^{\nu+1} - \left[\left(\frac{1}{a_P} \right)_f \left(\vec{\nabla} p_{rgh} \right)_f \right] \cdot \mathbf{S}_f \tag{3.25}$$

$$\begin{aligned} \Phi_f^{\nu+1} =& \Phi_f^{\nu+1} + \left[\left(\frac{1}{a_P} \right)_f \left[(-\nabla p)_f + (\mathbf{g} \cdot \mathbf{x})_f \left(\nabla {\rho_r}^{n+1} \right)_f - (\mathbf{g} \cdot \mathbf{x})_f \left(\nabla \rho(T)^{n+1} \right)_f \right. \right. \\ & \left. \left. + ({\rho_r}^{n+1} \mathbf{g})_f - (\rho(T)^{n+1} \mathbf{g})_f \right] \right] \cdot \mathbf{S}_f \end{aligned} \tag{3.26}$$

Finally, the velocity calculated at the center of the volume reads as,

$$\mathbf{v}^{\nu+1} = \mathbf{v}^{\nu+1} + \frac{1}{a_P} \mathcal{R} \left[\left(\Phi^{\nu+1} f - \Phi_u^{\nu+1} f \right) (a_P)_f \right] \tag{3.27}$$

where $\mathcal{R}$ is an operator used to recover cell-centered fields from fields given as fluxes at faces. Then, the static pressure, p, is reconstructed from p_{rgh}, leading the expression,

$$p = p_{rgh} + (\rho_r - \rho(T)) \mathbf{g} \cdot \mathbf{x} \tag{3.28}$$

3.3.6 Case Setup

Once the implementation is done, a first case is studied with the existing solver, *buoyantBoussinesqPimpleFoam*. The boundary conditions, thermophysical properties and some other solver parameters are described along the following subsections:

Boundary conditions

Five boundaries are defined in the current case:
Left: is considered a wall with a fixed value of temperature. This is the hot wall. No velocity is prescribed.
Right: considered to be the cold wall with a fixed temperature. No velocity is prescribed.
Top: this is considered the top wall and it is adiabatic, thus, no heat transfer is assumed and zero gradient is applied. No velocity is applied.
Bottom: This shares similar conditions as the top wall.
frontAndBack: this uses a symmetry plane condition in the z direction since the problem is considered to be 2-dimensional. For such boundary type, no more conditions need to be prescribed.

Thermophysical properties

Solver parameters

Boundary	Conditions
Left	$T_l = 283, v_l = 0$
Right	$T_r = 273, v_r = 0$
Top	$\frac{\partial T_u}{\partial n} = 0, v_u = 0$
Bottom	$\frac{\partial T_b}{\partial n} = 0, v_b = 0$

TABLE 3.1: Boundary conditions for natural convection case.

Water properties	Symbol	Values	Units
Density	ρ_r	999.8	$kg.m^{-3}$
Dynamic viscosity	μ	0.001003	$kg.m^{-1}.s^{-1}$
Thermal conductivity	λ	0.6	$W.m^{-1}.K^{-1}$
Heat capacity	C_p	4182	$J.kg.K^{-1}$
Gravitational acceleration	g	9.81	$m.s^{-2}$
Thermal diffusivity	γ	1.435e-7	$m^2.s^{-1}$
Thermal expansion coefficient	β	6.734e-5	K^{-1}
Laminar Prandtl number	P_r	6.99	-
Reference temperature	T_r	6.734e-5	K

TABLE 3.2: Water properties for natural convection.

Modeling Term	Keyword	Scheme	Remarks
Time derivatives	ddtSchemes	Euler	
Divergence term			
Gradient term	gradSchemes	Gauss linear	
Laplacian term	laplacianSchemes	Gauss linear uncorrected	
Others	snGradSchemes	uncorrected	
	interpolationSchemes	linear	

TABLE 3.3: Discretization schemes.

Equation	Linear Solver	Smoother/Preconditioner	Tolerance
Pressure correction equation	PCG	DIC	1e-8
Momentum equation	PBiCGStab	DILU	1e-6
Temperature equation	PBiCGStab	DILU	1e-6

TABLE 3.4: Solvers for the discretised equations.

Parameter	Value	Remarks
momentumPredictor	no	
nOuterCorrectors	1	
nNonOrthogonalCorrectors	0	
nCorrectors	2	

TABLE 3.5: Parameters for the discretised equations.

3.3.7 Validation of Results and Conclusions

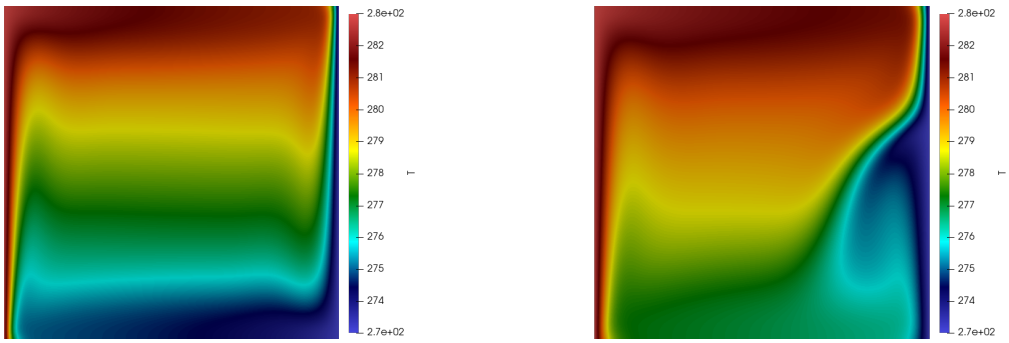

(A) Temperature magnitude comparison at t = 1500s. Left: BuoyantBoussinesqPimpleFoam. Right: NCMF

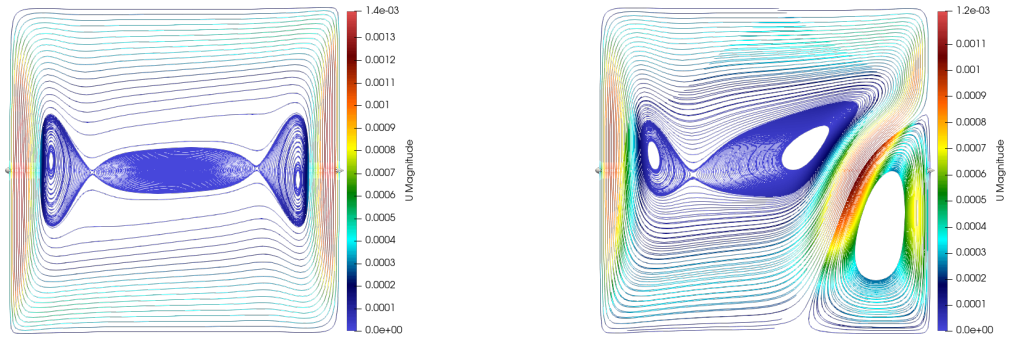

(B) Velocity magnitude comparison at t = 1500s. Left: BuoyantBoussinesqPimpleFoam. Right: NCMF

FIGURE 3.4: Comparison between BuoyantBoussinesqPimpleFoam and NCMF*

NCMF*: Natural convection modified solver.
In order to compare consistently the obtained results with those of the literature, the

following dimensionless values are pointed out:

$$\tilde{T} = \frac{T - T_{\text{cold}}}{T_{\text{hot}} - T_{\text{cold}}} = \frac{T - 273}{10} \tag{3.29}$$

$$\tilde{x} = \frac{x}{\ell} = \frac{x}{38 \times 10^{-3}} \tag{3.30}$$

$$\tilde{v} = \frac{v\ell}{\gamma} = \frac{v38 \times 10^{-3}}{1.435 \times 10^{-7}} \tag{3.31}$$

$$\tilde{u} = \frac{u\ell}{\gamma} = \frac{u38 \times 10^{-3}}{1.435 \times 10^{-7}} \tag{3.32}$$

$$\tilde{t} = \frac{t\gamma}{\ell^2} = \frac{t \times 1.435 \times 10^{-7}}{1.444 \times 10^{-6}} \tag{3.33}$$

$$\tilde{y} = \frac{y}{\ell} = \frac{y}{38 \times 10^{-3}} \tag{3.34}$$

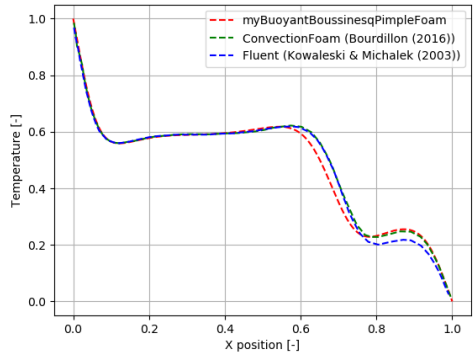

(A) Temperature along horizontal line.

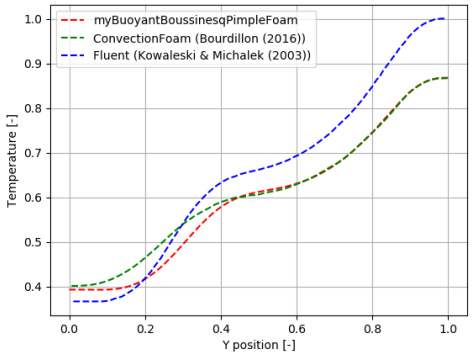

(B) Temperature along vertical line.

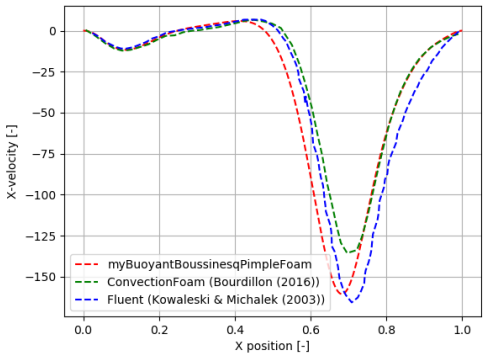

(C) U-velocity along horizontal line.

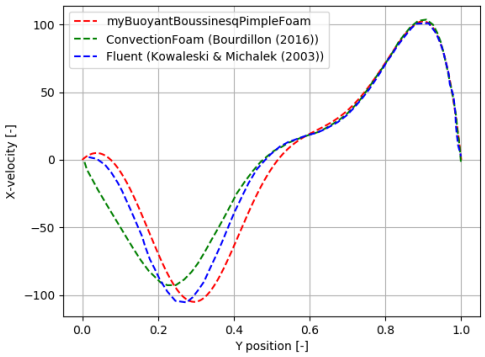

(D) U-velocity along vertical line.

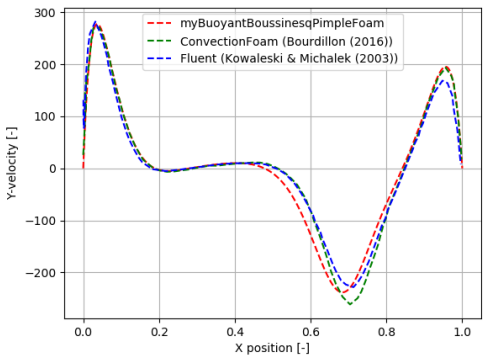

(E) V-velocity along horizontal line.

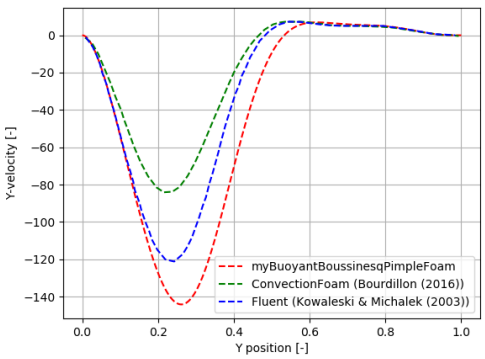

(F) V-velocity along vertical line.

FIGURE 3.5: Adimensional magnitudes comparison.

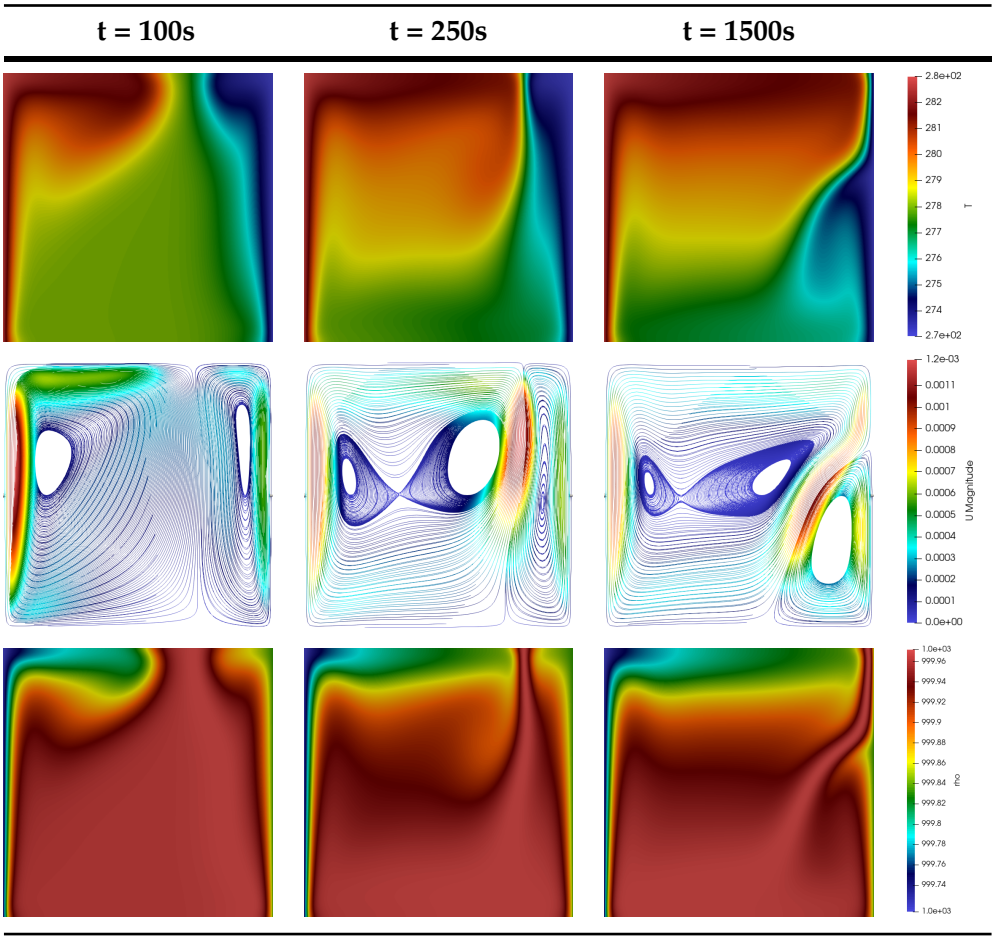

TABLE 3.6: Numerical results of Natural convection modified solver between $t = 100s$ and $1500s$.

3.4 OpenFOAM: IcoReactingMultiphaseInterFOAM. Phase-Change Process

The solidification process is assessed in the framework of an existing multiphase solver.

3.5 Case Description.

In the context of the solidification process, two regular geomtries are created: A squared and cylindrical plane geometries.

3.5.1 Hypotheses And Assumptions

To carry out the phase-transition process, some assumptions are taken into account so as to simplify the multiphysics ocurring during such arising phenomena.

Two phase properties

Within a multiphase framework, a model reflects a jump in properties through the interphase. Thus, a smooth transition between phase properties must be achieved.

$$\lambda = \lambda_\ell \alpha_\ell + \lambda_s f_s \tag{3.35}$$

$$C_p = C_{p_\ell} \alpha_\ell + C_{p_s} f_s \tag{3.36}$$

$$\mu = \mu_\ell \alpha_\ell + \mu_s f_s \tag{3.37}$$

In the case of polynomial density variation it is settled in a similar manner. The polynomial is not thought to suit negative temperatures, and when the problem is within this range, the density should take ice's density.

$$\rho(T)' = \rho(T) \alpha_\ell + \rho_s f_s \tag{3.38}$$

3.5.2 Governing Equations

The solution of the system of equations given by the multiphase solver relies on a pressure-velocity coupling loop based on PISO (*Pressure-Implicit with Splitting of Operators*). In order to give more stability to the solution and to simplify the boundary conditions, the pressure is treated by using a modified pressure:
Therefore, due to the commented before, the buoyancy terms appearing on the RHS of the momentum equation, are implemented on the pressure equation.

3.5.2.1 Momentum Equation

3.5.2.2 Energy Equation

3.5.3 Solver description. Control Loop

IcoReactingMultiphaseInterFoam solver is a multiphase, multicomponent incompressible solver based on volume of fluid method. The solver captures the interfaces and includes contact angle and surface tension effects for each phase. Moreover, this solver supports mass and heat transfer across phases.

3.5.4 Phase models

The solver presents three phase model types:

- **pureStaticSolidPhaseModel:** For pure static phase, like a solid.
- **pureMovingPhaseModel:** For pure moving phase, like a fluid.
- **multiComponentMovingPhaseModel:** For multi-component moving phase, like a multi-component fluid.

3.5.5 Mass transfer models

For each pair of phases, two mass transfer models might be used:

- **Lee model:** Used for solid melting and liquid solidification.
- **KineticGasEvaporation:** Used for condensation and evaporation.

In this thesis, only the Lee model will be considered for further explanation.

3.5.6 Code implementations

3.5.7 Case Setup

Boundary conditions

For the squared cavity: The initial conditions for the velocity and temperature fields are inherited from the last timestep of the natural convection case. *inletOutlet

Boundary	Conditions
Left	$\frac{\partial \alpha_l}{\partial n} = 0, \frac{\partial \alpha_s}{\partial n} = 0$
Right	$\alpha_l = inletOutlet * (1), \alpha_l = inletOutlet(0)$
Upper	$\frac{\partial \alpha_l}{\partial n} = 0, \frac{\partial \alpha_s}{\partial n} = 0$
Bottom	$\frac{\partial \alpha_l}{\partial n} = 0, \frac{\partial \alpha_s}{\partial n} = 0$

TABLE 3.7: Boundary conditions for natural convection case.

is normally the same as zero gradient but it switches to fixed value if the velocity vector next to the boundary aims inside the domain. For the cylinder:

Boundary	Conditions
Left	$T_l = 283, v_l = 0$
Right	$T_r = 273, v_r = 0$
Upper	$\frac{\partial T_u}{\partial n} = 0, v_u = 0$
Bottom	$\frac{\partial T_b}{\partial n} = 0, v_b = 0$

TABLE 3.8: Boundary conditions for natural convection case.

Water properties	Symbol	Values	Units
Water density	ρ_l	999.8	$kg.m^{-3}$
Ice density	ρ_s	916.8	$kg.m^{-3}$
Water kinematic viscosity	ν_l	1.79e-6	$m^2.s^{-1}$
Ice kinematic viscosity	ν_s	2.0e-6	$m^2.s^{-1}$
Water thermal conductivity	λ_l	0.56	$W.m^{-1}.K^{-1}$
Ice thermal conductivity	λ_s	2.26	$W.m^{-1}.K^{-1}$
Heat capacity	$C_{p_l} = C_{p_s}$	4202	$J.kg.K^{-1}$
Gravitational acceleration	g	9.81	$m.s^{-2}$
Thermal diffusivity	γ	1.435e-7	$m^2.s^{-1}$
Thermal expansion coefficient	β	6.734e-5	K^{-1}
Latent heat	L	335000	$J.K^{-1}$
Laminar Prandtl number	P_r	6.99	-
Reference temperature	T_r	6.734e-5	K
Darcy's constant	D_c	10e8	-

TABLE 3.9: Water properties for natural convection.

Water nucleation properties	Symbol	Values	Units
Planck constant	h	6.63e-34	$J.s$
Boltzmann constant	k_B	1.38e-23	$J.K^{-1}$
Gibbs free energy	Δ_{gv}	4e-20	J
Interfacial tension	γ_{yw}	2.91e-2	$J.m^{-2}$
Latent heat per volume	H_{lv}	3.10e8	$J.m^{-3}$
Shape coefficient of nucleation	α_{ey}	0.0001	-
Water molecule per volume	n_L	5.5e4	m^3

TABLE 3.10: Water properties for solidification.

Modeling Term	Keyword	Scheme	Remarks
Time derivatives	ddtSchemes		
Divergence term			
Gradient term	gradSchemes		
Laplacian term	laplacianSchemes		
Others	snGradSchemes		
	interpolationSchemes		

TABLE 3.11: Discretization schemes.

Thermophysical properties

Solver parameters

3.5.8 Validation of Results and Conclusions

The validation of the phase change problem is achieved by different methodologies. First, the enthalpy-porosity method is compared with available data found in the thesis of Bourdillon, 2016 and KOWALEWSKI and REBOW, 1999. For the Lee model based on the *Classical Nucleation Theory*, the results are validated against the analytical solution given by the Neumann solutions of the Stefan problem.

Equation	Linear Solver	Smoother/Preconditioner	Tolerance
Pressure correction equation	PCG	DIC	
Momentum equation	smoothSolver	symGaussSeidel	
Volume fraction equation	smoothSolver	symGaussSeidel	

TABLE 3.12: Solvers for the discretised equations.

Parameter	Value	Remarks
nAlphaCorr	PCG	DIC
nAlphaSubCycles	smoothSolver	symGaussSeidel
cAlpha	smoothSolver	symGaussSeidel
momentumPredictor		
nOuterCorrectors		
nNonOrthogonalCorrectors		
nCorrectors		

TABLE 3.13: Parameters for the discretised equations.

3.5.8.1 Stefan Problem

The Stefan problem, is an initial boundary value problem of a parabolic differential equation with discontinuous coefficients on the phase transitions interfaces [Vasilyev and Vasilyeva, 2020]. The analytical solution to the classical Stefan problem exists in a limited range of idealized situations. Some of them involve semi-infinite or infinite regions with simple and boundary conditions. Based on the work of Vasilyev and Vasilyeva, 2020 and Zhao, Zhao, and Xu, 2018, a two-region solidification process in a semi-infinite region is used to study the feasibility of the VOF-Lee model based on the Nucleation Theory.

One-dimensional problem

In seek of simplification, and recalling the 1D problem as shown in the figure: the initial conditions are expressed as:

$$u_0(x) = u_0, \quad t = 0, \quad x \in [0, L], \tag{3.39}$$

while the boundary conditions are the shown below:

$$u(0,t) = -15C, \quad \frac{\partial u}{\partial x}(L,t) = 0, \quad t > 0 \tag{3.40}$$

The discontinuous exact solutions are:

$$\begin{cases} T_l(x,t) = \dfrac{\operatorname{erfc}\left(\frac{x}{2\sqrt{a_1 t}}\right)}{\operatorname{erfc}\left(\lambda\sqrt{\frac{a_s}{a_1}}\right)}(T_m - T_0) + T_0, & x > \xi(t), \\ T_s(x,t) = \dfrac{\operatorname{erf}\left(\frac{x}{2\sqrt{a_s t}}\right)}{\operatorname{erf}\cdot^{\sim}}(T_m - T_b) + T_b, & x \le \xi(t). \end{cases} \tag{3.41}$$

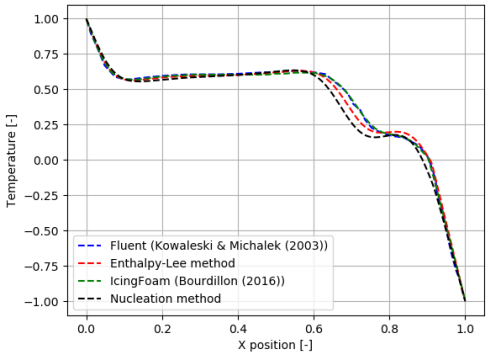

(A) Temperature along horizontal line.

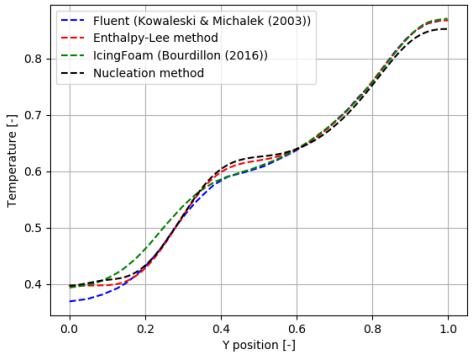

(B) Temperature along vertical line.

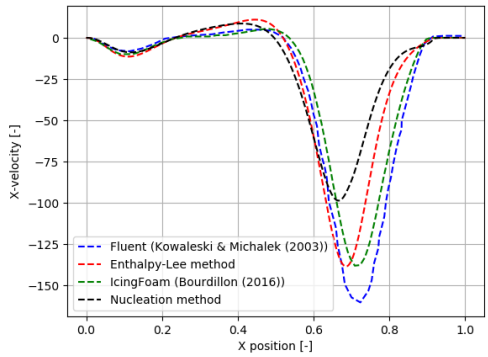

(C) U-velocity along horizontal line.

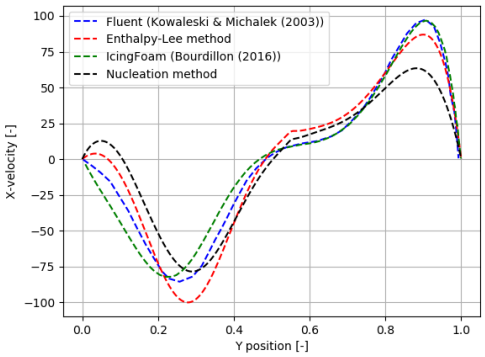

(D) U-velocity along vertical line.

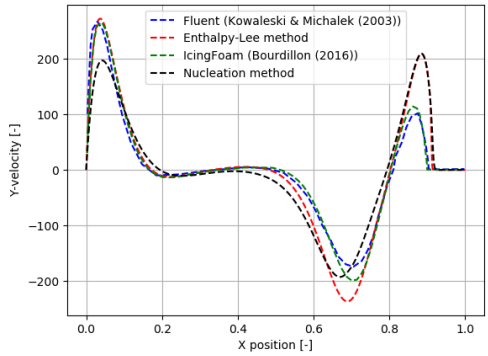

(E) V-velocity along horizontal line.

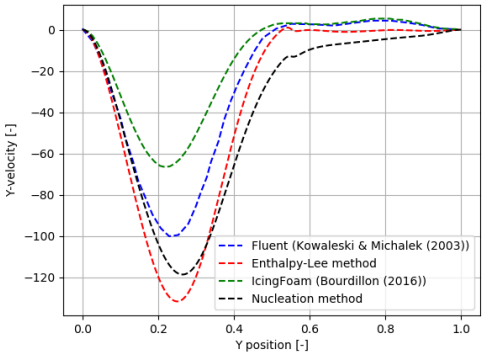

(F) V-velocity along vertical line.

FIGURE 3.6: Adimensional magnitudes comparison.

By using a phase change interface condition, a solution to the trascendental equation may be found:

$$\frac{e^{-\lambda^2}}{\operatorname{erf}(\lambda)} + \frac{k_l}{k_s}\sqrt{\frac{a_s}{a_1}}\frac{T_m - T_0}{T_m - T_b}\frac{e^{-\frac{a_s}{a_1}\lambda^2}}{\operatorname{erfc}\left(\lambda\sqrt{\frac{a_s}{a_1}}\right)} = \frac{\lambda L\sqrt{\pi}}{c_{ps}\left(T_m - T_b\right)} \tag{3.42}$$

The secant method is used as the iterative scheme to find the root of the given function with $tol < 1e-12$. The root of γ is 0.2204835149063661

3.5.8.2 Interface height

The evolution of the interface is:

$$X(t) = 2\lambda\sqrt{a_s t} \tag{3.43}$$

Chapter 4

Numerical Simulation of Heat Transfer

4.1 OpenFOAM: chtMultiphaseInterFOAM. Conjugate Heat Transfer

The last objective of this thesis is to extend the multiphase solver of the previous section so it can account for multiregion purposes. To do so, a new solver derived from the concept of an existing multiregion solver is implemented. The existing solver, *chtMultiRegionFoam* is developed on the basis that the fluid it solves undergoes the compressible Navier-Stokes equations with buoyancy forces and the energy equation per unit mass with gravity terms as follows:

Continuity Equation

$$\frac{\partial \rho}{\partial t} + \nabla \cdot (\rho \boldsymbol{u}) = 0 \tag{4.1}$$

Momentum Equation

$$\begin{aligned} &\frac{\partial \rho \boldsymbol{u}}{\partial t} + \nabla \cdot (\rho \boldsymbol{u} \otimes \boldsymbol{u}) = \\ &-\nabla p_{\text{rgh}} + \nabla \cdot \left[\mu \left\{ \nabla \otimes \boldsymbol{u} + (\nabla \otimes \boldsymbol{u})^{\text{T}} \right\} \right] - \nabla \left(\frac{2}{3} \mu \nabla \cdot \boldsymbol{u} \right) - \boldsymbol{g} \cdot \boldsymbol{x} \nabla \rho \end{aligned} \tag{4.2}$$

Energy Equation

$$\frac{\partial \rho h}{\partial t} + \nabla \cdot (\rho \boldsymbol{u} h) + \nabla \cdot (\rho \boldsymbol{u} K) = \nabla \cdot \left(\frac{\lambda}{c_p} \nabla h \right) + \rho \boldsymbol{u} \cdot \boldsymbol{g} \tag{4.3}$$

where $\boldsymbol{u}$ is the velocity vector, h is the enthalpy, $K = 0.5^{*}\boldsymbol{u} \cdot \boldsymbol{u}$ is the kinetic energy per unit mass, $p_{rgh} = p - \rho \boldsymbol{g} \cdot \boldsymbol{x}$ the modified pressure so that the momentum equation accounts for the buoyancy terms, and the remaining thermophysical properties, μ, λ, C_p being the kinematic viscosity, the thermal conductivity and the specific heat accordingly. The energy equation does not include radiation, heat generation term and chemical reaction.
Therefore, the challenge of this part is to couple the multiphase solver (*IcoReactingMultiPhaseInterFoam*) that allows for the solving of a fluid undergoing phase-change with a solid region.

4.1.1 Case description

4.1.2 Hypotheses And Assumptions

4.1.3 Governing Equations of the Fluid Region

4.1.4 Governing Equations of the Solid Region

4.1.4.1 Energy Equation

$$\nabla \cdot \left(\frac{\lambda}{\rho c_p} \nabla h \right) = 0 \tag{4.4}$$

4.1.5 Solver description. Control Loop

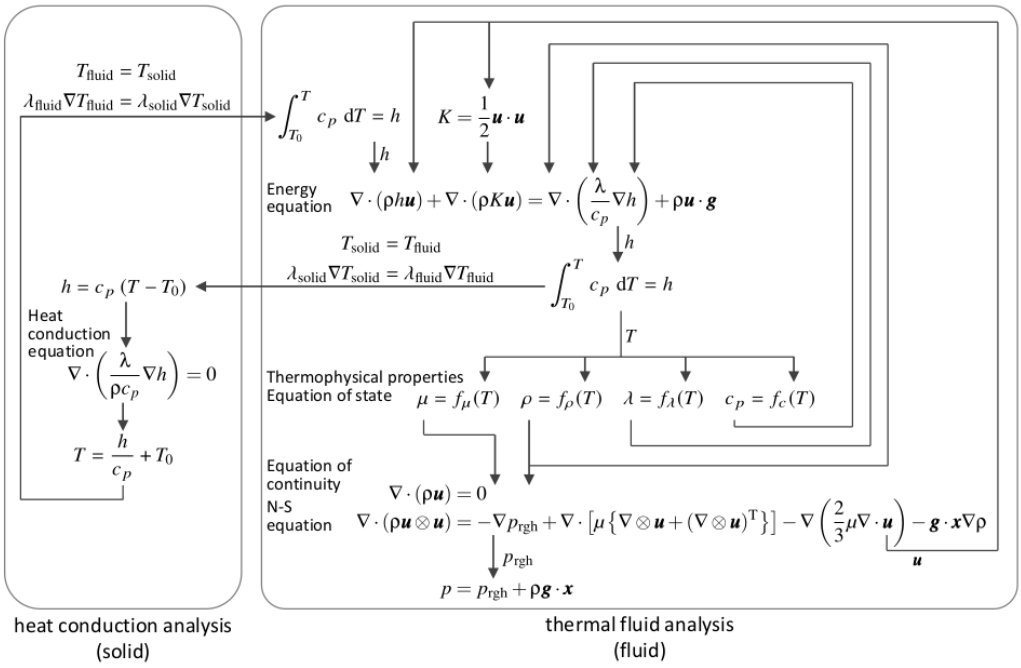

FIGURE 4.1: Flowchart of the conjugate heat transfer solver.**sugimoto_kuramae_matsumoto_watanabe_2021**

chtMultiphaseInterFoam is a new solver derived from the existing solver chtMultiRegionFoam. It is implemented to cope with transient fluid flow and solid heat conduction with conjugate heat transfer between regions. The solution follows a sequential strategy: equations of the fluid are first solved using the temperatures of the solid of the preceding loop to set the boundary conditions for the fluid part.Then, the equation for the solid is solved with the temperatures of the fluid to define lately the boundary conditions of the solid. This process is iteratively executed until convergence is reached.

4.1.6 Code implementations

4.1.7 Case Setup

4.1.7.1 Boundary conditions

At the interface between solid and liquid regions, it is required to set an appropriate boundary condition which couples the energy equations in these areas. Considering two cells at each side of the interface such as in the Figure where T_c and T_p is the temperature at the cell center and on the patch (2D boundary) accordingly. q_1 is the heat flux going out of the $cell_1$ and q_2 the heat flux entering the $cell_2$. The energy conservation in this zone constrains the temperature and heat fluxes to be equat at both sides of the interface. Then, temperature, in magnitude yields as

$$T_{p,1} = T_{p,2} = T_p, \tag{4.5}$$

and as well, for the fluxes

$$q_1'' = q_2'' = q'' \tag{4.6}$$

while the magnitude for the heat fluxes is derived from the one-dimensional expression for the Fourier's law and it gives

$$-k_1 \frac{\partial T}{\partial n}\bigg|_{\text{side 1}} = -k_2 \frac{\partial T}{\partial n}\bigg|_{\text{side 2}} \tag{4.7}$$

where κ is the termal conductivity and n the direction normal to the patch. Discretizing linearly the temperature gradient of the previous equation, and with respect of the scheme of the Figure [], the differential equation that yields

$$k_1 \Delta_1 \left(T_{c,1} - T_p\right) = k_2 \Delta_2 \left(T_p - T_{c,2}\right) \tag{4.8}$$

where the temperatures and fluxes at the center of the patches are described as

$$\begin{aligned} T_p &= \frac{k_1 \Delta_1 T_{c,1} + k_2 \Delta_2 T_{c,2}}{k_1 \Delta_1 + k_2 \Delta_2} \\ q'' &= k_1 \Delta_1 \left(T_{c,1} - T_p\right) = k_2 \Delta_2 \left(T_p - T_{c,2}\right). \end{aligned} \tag{4.9}$$

4.1.8 Validation of Results and Conclusions

Chapter 5

Conclusions

Chapter 6

Future Works

Appendix A

A.1 Enthalpy-porosity library

A.2 Lee-Nucleation library

A.3 chtMultiphaseInterFoam solver

The color of links can be changed to your liking using:
`\hypersetup{urlcolor=red}`, or
`\hypersetup{citecolor=green}`, or
`\hypersetup{allcolor=blue}`.
If you want to completely hide the links, you can use:
`\hypersetup{allcolors=.}`, or even better:
`\hypersetup{hidelinks}`.
If you want to have obvious links in the PDF but not the printed text, use:
`\hypersetup{colorlinks=false}`.

Bibliography

Bourdillon, Arnaud (2016). "investigation towards a coupling between population balance and solidification models". PhD thesis. Cranfield University.

Huang, Chengyu, Wenhua Wang, and Weizhong Li (2020). "A Novel 2D Model for Freezing Phase Change Simulation during Cryogenic Fracturing Considering Nucleation Characteristics". In: *Applied Sciences* 10.9, p. 3308. DOI: 10.3390/app10093308.

Ickes, Luisa et al. (2015). "Classical nucleation theory of homogeneous freezing of water: thermodynamic and kinetic parameters". In: *Physical Chemistry Chemical Physics* 17.8, pp. 5514–5537. DOI: 10.1039/c4cp04184d.

KOWALEWSKI, T. A. and M. REBOW (1999). "Freezing of Water in a Differentially Heated Cubic Cavity". In: *International Journal of Computational Fluid Dynamics* 11.3-4, pp. 193–210. DOI: 10.1080/10618569908940874.

Vasilyev, Vasily and Maria Vasilyeva (2020). "An Accurate Approximation of the Two-Phase Stefan Problem with Coefficient Smoothing". In: *Mathematics* 8.11, p. 1924. DOI: 10.3390/math8111924.

Wu, Daoyong, Yuanming Lai, and Mingyi Zhang (2015). "Heat and mass transfer effects of ice growth mechanisms in a fully saturated soil". In: *International Journal of Heat and Mass Transfer* 86, pp. 699–709. DOI: 10.1016/j.ijheatmasstransfer.2015.03.044.

Zhao, Y., C.Y. Zhao, and Z.G. Xu (2018). "Numerical study of solid-liquid phase change by phase field method". In: *Computers Fluids* 164, pp. 94–101. DOI: 10.1016/j.compfluid.2017.05.032.